A new deterministic CA model for traffic flow with multiple states

1999 J. Phys. A: Math. Gen. 32 93

(http://iopscience.iop.org/0305-4470/32/1/010)

J. Phys. A: Math. Gen. **32** (1999) 93–104. Printed in the UK PII: S0305-4470(99)95382-9

A new deterministic CA model for traffic flow with multiple states

Katsuhiro Nishinari†§ and Daisuke Takahashi‡‖

† Department of Mechanical Engineering, Faculty of Engineering, Yamagata University, Yonezawa, Yamagata 992, Japan

‡ Department of Mathematical Sciences, Waseda University, Ohkubo 1-6-9, Shinjuku-ku, Tokyo 169, Japan

Received 29 June 1998, in final form 8 September 1998

Abstract. In this paper, an ultra-discrete version of Burger's equation, which includes the rule-184 CA model, is extended to treat a higher velocity. The extended model has multiple states at the transition region of car density from free to congested phase in the fundamental diagram. The state of free phase at high density is unstable under perturbation, and its stability is discussed in detail.

1. Introduction

Traffic flow is a complex discrete system and its analysis is one of main themes in complex system theory. It shows interesting collective behaviours, such as pattern formation, phase transition and scale-invariant fluctuations. The system has been studied by many different approaches, which can be broadly divided into two categories; macroscopic and microscopic. Macroscopic approaches are based on hydrodynamical equations [1, 2]. In these approaches, we need an empirical steady flow-density relation from some observed data in order to analyse time evolution of traffic flow. A flow versus density diagram of steady states is called a fundamental diagram.

In order to explain the diagram itself, we use microscopic approaches instead of macroscopic ones. Microscopic approaches are called car-following theory, because a behaviour of each vehicle is modelled in relation to a vehicle ahead. First, Newell introduced a preferred velocity function and obtained a differential delay equation [3]. Recently, an optimal-velocity model was proposed by Bando *et al* [4], and they introduced a semi-empirical function of desirable velocity depending on headway distance. They also obtained a fundamental diagram, in which they can successfully show the existence of discontinuity at a critical density of transition from free to congested flow [5]. We show here an example of a flow versus occupancy diagram of observed data taken by the Japanese Public Highway Corporation [6] (figure 1). We find a discontinuity at the occupancy ∼25%, and there seems to exist multiple states around the critical occupancy. Many other real diagrams show this type of graph and the flow-density curve has the shape of 'inverse λ' [6]. This discontinuity has been explained by many researchers. Edie introduced a discontinuity by hand by using Greenberg's model

§ E-mail address: knishi@dips.dgw.yz.yamagata-u.ac.jp

‖ E-mail address: daisuke@mse.waseda.ac.jp

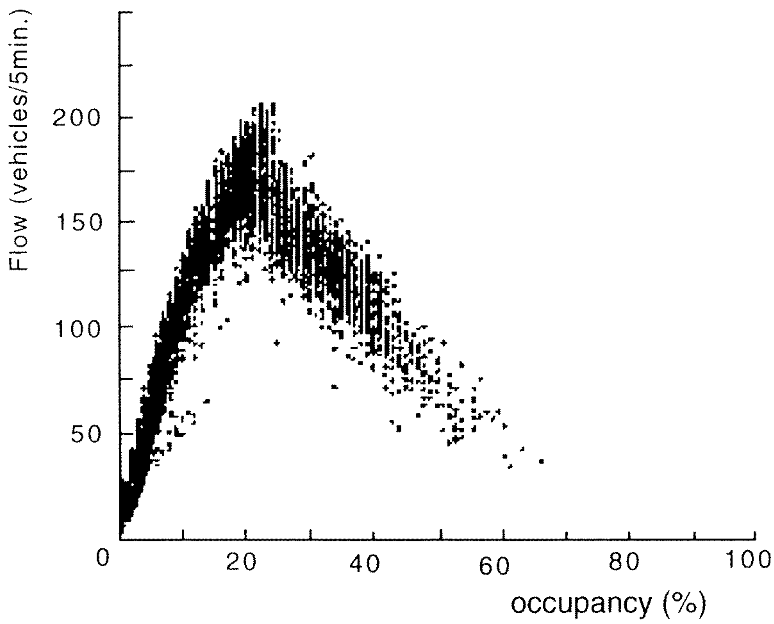

Figure 1. The observed data of flow (vehicles/5 min) versus occupancy of the road. This diagram was produced by the Japanese Public Highway Corporation.

[7]. Navin and Hall proposed a three-dimensional space of data, i.e. relating flow, velocity and density, and explained the discontinuity by using catastrophe theory [8].

A more recent development of traffic flow theory is the cellular automaton (CA) model. The CA model is quite simple, has flexibility, and is suitable for computer simulations of discrete phenomena [9]. Nagel and Schreckenberg (NS) proposed a stochastic traffic CA for the description of single-lane highway traffic. The NS model is able to reproduce the spontaneous formation of jams by introducing braking probability in its evolutional rule [10, 11]. Fukui and Ishibashi introduced a deterministic CA model by using rule-184 CA [12]. Fukś and Boccara also proposed deterministic CA models by extending the rule-184 CA [13]. Rule-184 CA is famous and widely used as a prototype deterministic model of traffic flow. The fundamental diagram of the NS model does not show discontinuity at a critical density [14, 15]. Those deterministic models that use the rule-184 CA also do not show such discontinuity or multiple states, even though they exhibit sharp phase transition [13]. A CA model showing discontinuity was obtained first in [16]. In that model, a so-called 'slow-to-start' rule was introduced and led to multiple states in the fundamental diagram. In [17, 18], a slow-to-start rule was introduced probabilistically by considering that standing cars accelerate with lower probability than moving cars. Those models are generalizations of the NS model, and the existence of metastable states is shown in a density region close to the maximum flow.

Recently an ultradiscrete version of Burger's equation, that is, Burger's cellular automaton (BCA) has been proposed and used as a particle hopping model [19]. BCA is shown to contain rule-184 CA as a special case, and thus is considered as a generalization of rule-184 CA. In this paper, we extend BCA to treat a higher velocity, and we find that our new deterministic CA model shows multiple states at a transition region in the fundamental diagram. Our model is fully deterministic and suitable for detailed study of the properties of discontinuity and multiple states in the diagram.

This paper is organized as follows. BCA is introduced as a traffic flow model and its properties and problems are discussed in section 2. BCA is extended to treat a higher velocity and a fundamental diagram is analysed in section 3. In section 4, unstable free flow is studied in detail and concluding discussions are given in section 5.

2. BCA as a traffic flow model

2.1. A new CA model of traffic flow

BCA is given by [19]

$$U_j^{t+1} = U_j^t + \min(M, U_{j-1}^t, L - U_j^t) - \min(M, U_j^t, L - U_{j+1}^t). \tag{1}$$

It has been shown in [19] that (1) is related to Burger's equation $v_t = 2vv_x + v_{xx}$ through the transformation $U_j^t = L/2 + \varepsilon\Delta x v(j\Delta x, t\Delta t)$, where Δx and Δt are lattice intervals in x and t respectively and ε is a parameter used in the ultradiscrete formula [20]. There are two parameters L and M in BCA. In our previous paper [19], we showed the following properties of this equation: assuming that $M > 0$, $L > 0$ and $0 \leqslant U_j^t \leqslant L$ for any site j at a certain time t, then, $0 \leqslant U_j^{t+1} \leqslant L$ holds for any j. Thus (1) is equivalent to a CA with a value set $\{0, 1, \ldots, L\}$ under the above conditions. Moreover, if we put a restriction $L \leqslant M$ and $L = 1$ on BCA, then BCA is equivalent to rule-184 CA, which is used as a prototype of traffic flow models [12].

It is, therefore, natural to consider (1) with general L and M as a traffic model. The road is expressed by a space of discrete sites indexed by a site number j. We assume that the capacity of each site is L cars. U_j^t denotes the number of cars at site j and time t, which is an integer from 0 to L. Cars at site j and time t stay at site j or move to site $j+1$ at the next time $t+1$. The maximum number of movable cars is M. Under this restriction, they move to fill vacant spaces at site $j+1$. The second and the last term of the right-hand side of (1) represents the number of cars that comes from the site $j-1$ and moves to the next site $j+1$, respectively. It is apparent that the total number of cars is preserved under the rule.

The physical meaning of this model may be interpreted in two ways: first, the road can be seen as an L-lane freeway in a coarse sense, and the effect of lane changes by cars is not considered explicitly; second, we can consider it as a single-lane freeway where $\rho_j^t = U_j^t/L$ represents the local density of cars at site j and time t. If we choose large L, the local density can take detailed values from 0 to 1. In the latter case, the number U_j^t itself no longer represents the real number of cars at site j. Using the second interpretation, we define ρ by an average density of cars per site given by

$$\rho \equiv \frac{1}{K}\sum_{j=1}^{K} \rho_j^t \tag{2}$$

where we consider a periodic boundary condition to the road and K is its period. We consider that throughout this paper the road is periodic, or a circuit. Since the total number of cars is preserved, the density ρ is constant during the course of time. In order to describe the fundamental diagram, we define an average flow of cars by

$$q^t \equiv \frac{1}{KL}\sum_{j=1}^{K} \min(M, U_j^t, L - U_{j+1}^t). \tag{3}$$

By using (3) and (2), the fundamental diagram is shown in figure 2 in the case $L \leqslant 2M$. The diagram shows steady-state, long-time averages over the entire system starting from random initial conditions. The flow q^t becomes constant at large enough t. In a region of $\rho < \frac{1}{2}$, all

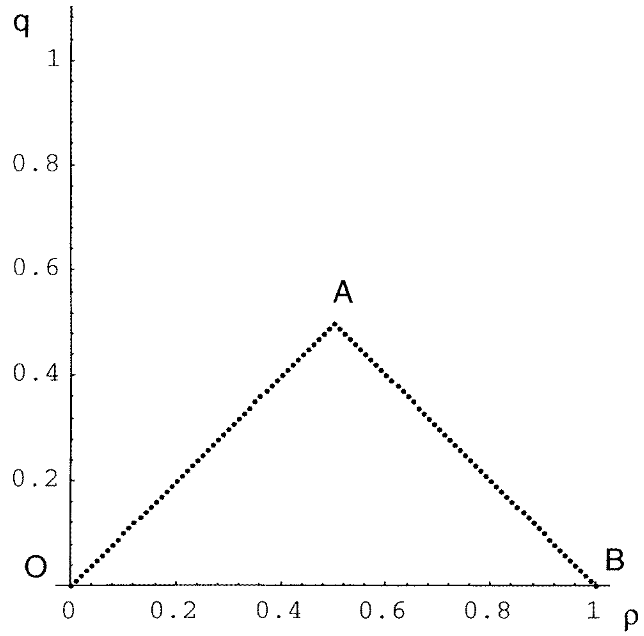

Figure 2. The fundamental diagram in the case $L = 2$ of BCA. The number of samples is 1000 and the system size used for the simulation is $K = 50$.

dots are exactly on a line $q = \rho$, and on a line $q = 1 - \rho$ in a region of $\rho > \frac{1}{2}$ from any initial data. These facts have been proved by using an ultradiscrete diffusion equation [19]. There is a sharp transition point $\rho = \frac{1}{2}$ which separates free laminar flow and congested flow. The fundamental diagram in figure 2 is unique for any L and M ($L \leqslant 2M$), especially it is the same as that of rule-184 CA ($L = 1$).

In the case of $L > 2M$, the shape is trapezoidal (figure 3). The steady flow of the region of the density $M/L \leqslant \rho \leqslant (L - M)/L$ has the constant value M/L. This result has also been proved in [19] in relation to a particle model. It should be noted that the trapezoid shape is similar to that of Yukawa *et al* [21], who introduced a blockage site artificially into the rule-184 CA to take a flow bottleneck into account. The blockage site has some transmission probability in their model. Our model, however, is fully deterministic and contains a parameter M in the role of flow limiter.

2.2. Properties and problems of BCA as a traffic model

In this subsection, we restrict ourselves to the case of $L \leqslant 2M$ and $L = 2$ for simplicity and investigate detailed properties of BCA. We have seen above that rule-184 CA and BCA show the same fundamental diagram. However, we should point out an important fact of BCA that multiple states are degenerated in the diagram. First, it is easily shown that BCA with $L = 2$ contains the rule-240, -184, -170 CA's [9] as a special case. In the case of $U_j^t \in \{0, 1\}$ for all j, from (1) the truth value table of BCA is expressed symbolically by

$$\frac{U_{j-1}^t U_j^t U_{j+1}^t}{U_j^{t+1}} = \frac{000}{0}, \frac{001}{0}, \frac{010}{0}, \frac{011}{0}, \frac{100}{1}, \frac{101}{1}, \frac{110}{1}, \frac{111}{1}.$$

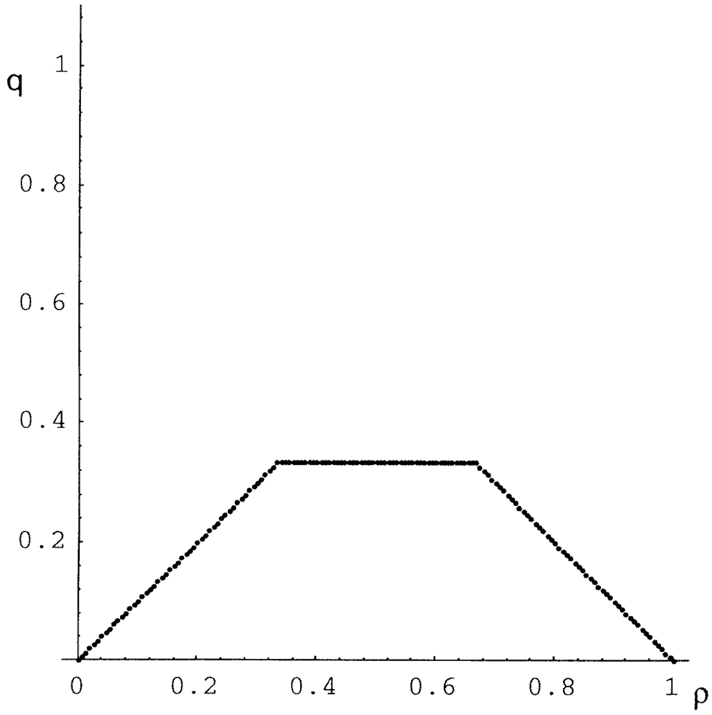

Figure 3. The fundamental diagram in the case $L = 3$ and $M = 1$ of BCA. The number of samples is 1000 and $K = 50$.

Then we see that $U_j^t \in \{0, 1\}$ for all t. This is nothing but the rule-240, and all patterns of '0' and '1' shift to the right. Next, in the case $U_j^t \in \{0, 2\}$ we obtain

$$\frac{U_{j-1}^t U_j^t U_{j+1}^t}{U_j^{t+1}} = \frac{000}{0}, \frac{002}{0}, \frac{020}{0}, \frac{022}{2}, \frac{200}{2}, \frac{202}{2}, \frac{220}{0}, \frac{222}{2}.$$

This is rule-184 of a value set $\{0, 2\}$. In the case $U_j^t \in \{1, 2\}$ we obtain

$$\frac{U_{j-1}^n U_j^n U_{j+1}^n}{U_j^{n+1}} = \frac{111}{1}, \frac{112}{2}, \frac{121}{1}, \frac{122}{2}, \frac{211}{1}, \frac{212}{2}, \frac{221}{1}, \frac{222}{2}.$$

This is rule-170, and all patterns of '1' and '2' shift to the left.

Thus in rule-240 CA, all cars expressed by the number '1' move right by one site in unit time in the background of 0's. All states constructed only from 0's and 1's are always less than $\frac{1}{2}$ density and therefore plotted on line O–A in figure 2. Similarly, in the rule-170 CA, the number '2', which stands for a full-packed site, propagates left in the background of 1's. The density of this case is always greater than $\frac{1}{2}$ and it is apparent that all states are plotted on the line A–B. Steady states containing only '2' and '0' are spread on the 'hat' O–A–B, which is proved in [19]. Therefore, the line O–A contains at least two kinds of steady states, i.e. those of rule-240 and rule-184. The line A–B also contains steady states of rule-170 and rule-184. Therefore it is found that steady states governed by different rules have the same traffic flow and car density in the BCA model. We call this situation 'degenerated' in this paper. This is a crucial difference between BCA with $L \geqslant 2$ and BCA with $L = 1$ (rule-184 CA). This fact plays an important role in the following sections.

BCA is, however, too simple to analyse the complexity of a congested flow. From figure 1 mentioned in section 1, the real flow does not show continuous transition from free to congested flow, but there is a discontinuity around the critical density, and flow q has multiple values at the same density ρ in the transition region. Although the fundamental diagram of figure 2 shows the phase separation of the free-moving region and the congested region, BCA is too simple to capture the nature of the transition from free to congested flow.

3. Extended BCA model

In the previous section, we saw that multiple states are degenerated at the same value of ρ in BCA. We show in the following that the degenerated states lead to remarkable changes in the fundamental diagram when we introduce higher velocities of cars. For the rule-184 CA model, the extension to higher velocities has been done by Fukui and Ishibashi [12], and they have shown that the critical density in the fundamental diagram becomes lower for the higher velocities. However, the fundamental diagram in their model does not show discontinuity at the critical density.

Let us define the velocity V as the maximum number of sites by which a car can advance in unit time. BCA is the case $V = 1$. We extend BCA to $V = 2$ in the following, and let us call this model 'extended BCA' (EBCA) in this paper. Following [12], we assume that a car can advance by two sites per time step if the successive two sites are not fully occupied. The rule for shifting cars per time step is given as follows: First, we consider that cars moving two sites have priority over those moving one site. Then the number of cars at site j that can move two sites forward is given by $a_j^t \equiv \min(U_j^t, L - U_{j+1}^t, L - U_{j+2}^t)$, where $L - U_{j+1}^t$ and $L - U_{j+2}^t$ represent the vacant spaces at the sites $j+1$ and $j+2$, respectively. Moreover, let us define the maximum number of cars at site j that can move as $b_j^t \equiv \min(U_j^t, L - U_{j+1}^t)$. Then cars that move only one site forward is given by $\min(b_j^t - a_j^t, L - U_{j+1}^t - a_{j-1}^t)$, where $L - U_{j+1}^t - a_{j-1}^t$ represents vacant space after all the cars moving two sites have moved. All sites are updated synchronously under this rule. Therefore, considering the number of cars entering into and escaping from site j, the evolutional rule of EBCA is given by

$$\begin{aligned} U_j^{t+1} &= U_j^t + a_{j-2}^t - a_j^t + \min(b_{j-1}^t - a_{j-1}^t, L - U_j^t - a_{j-2}^t) \\ &\quad - \min(b_j^t - a_j^t, L - U_{j+1}^t - a_{j-1}^t) \\ &= U_j^t + \min(b_{j-1}^t + a_{j-2}^t, L - U_j^t + a_{j-1}^t) - \min(b_j^t + a_{j-1}^t, L - U_{j+1}^t + a_j^t). \end{aligned} \quad (4)$$

Note that (4) includes the model of Fukui and Ishibashi [12] as a special case if we take $L = 1$. In this paper, for the sake of simplicity, we do not consider the flow-limiter M in this new model (4).

Let us analyse the traffic flow described by (4). The flow is defined by

$$q^t \equiv \frac{1}{KL} \sum_{j=1}^{K} \min(b_{j-1}^t + a_{j-2}^t, L - U_j^t + a_{j-1}^t). \quad (5)$$

In the following we restrict ourselves to the case $L = 2$. The fundamental diagram for this rule is given in figure 4. If we choose all the possible combinations of 0,1 and 2 as initial conditions, we obtain the diagram shown in figure 4(*a*). Figure 4(*b*) also shows the fundamental diagram of (4), but it is plotted by a finite number of random initial conditions. In both cases, we can see discontinuity around the transition region. The steady state line no longer has a hat shape but instead an 'inverse λ' shape, which is similar to that of real traffic flow given in figure 1, if we average fluctuations. In figure 4(*a*) we see that there are two steady states, i.e. free and congested, in the transition region $\frac{1}{3} \leqslant \rho \leqslant \frac{1}{2}$. In figure 4(*b*), the free-flow line is shorter

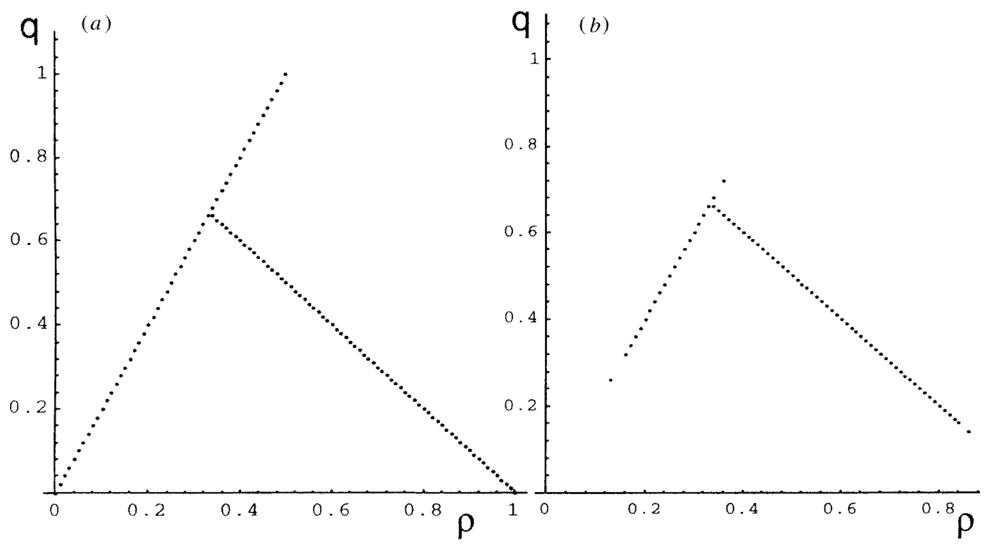

Figure 4. The fundamental diagram of EBCA. We set $K = 50$ and initial conditions are given by (*a*) all possible states of 0, 1 and 2; (*b*) a finite random states of 1000 samples.

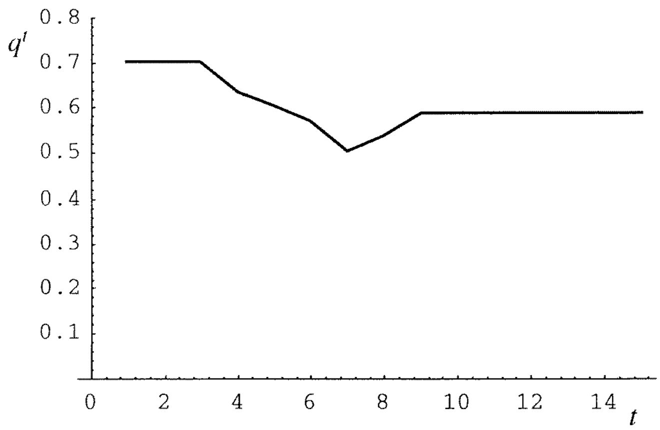

Figure 5. Typical time evolution of the flow of EBCA in the region $\frac{1}{3} \leqslant \rho \leqslant \frac{1}{2}$. The system size is $K = 50$.

compared with that of figure 4(*a*). This indicates that the states of high flow are highly ordered and therefore cannot be reached starting from random initial conditions, and the possibility of realizing free steady states near $\rho \sim \frac{1}{2}$ is small. Such states of high flow, although they are rarely observed in a real traffic flow, are important in considering the transition from free to congested flow. It is an advance of our model that we can prepare special initial configurations for generating high flux, and behaviours of them will be discussed in the next section.

It should be noted that the evolution of the flow can show damping oscillation (figure 5) in the course of time starting from random initial conditions in the region $\frac{1}{3} \leqslant \rho \leqslant \frac{1}{2}$, although it monotonously increases outside this region. In the BCA case, it is proved that the flow monotonously increases at any ρ [19]. We will consider why this oscillation occurs in EBCA in the next section.

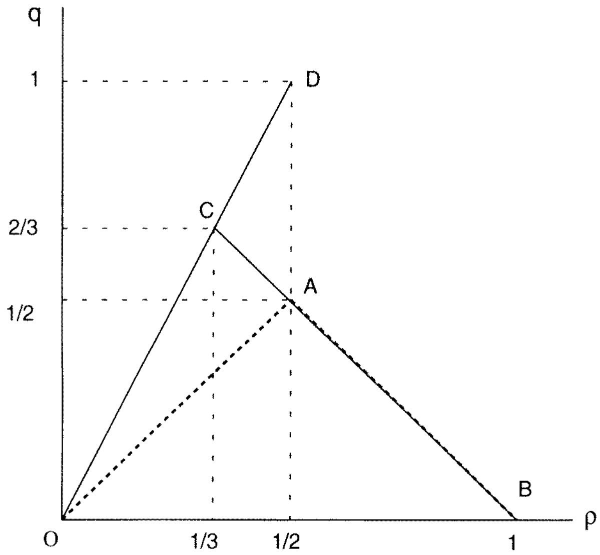

Figure 6. The schematic diagram of figures 1 and 4(*a*). The hat OAB represents the fundamental diagram of BCA and the lines OD and CB represents that of EBCA.

Let us explain why the multiple states appear when higher velocity is introduced. Figure 6 shows a schematic diagram of figure 4(*a*). The dotted line O–A–B represents the fundamental diagram of BCA which is given in figure 2. As mentioned above, two kinds of steady states are degenerated on the line in the case of BCA with $L = 2$. For example, in BCA two states are degenerated on the point A: ... 111111111 ... and ... 2020202020 ... if K is even. When we consider the higher velocity, these states separate into D and A respectively in figure 6. This is because the state ... 2020202020 ... cannot increase its velocity due to the full-packed '2' sites, although the state ... 111111111 ... can. Similarly, it is apparent that states consisted of '0' and '1', which are on the line O–A in BCA, will shift to line O–D in EBCA. Therefore, the slope of O–D is 2, while that of O–A in BCA is 1, and these slopes represent the maximum speed of each model.

Next, we consider states consisting of '0' and '2'. These are on the hat O–A–B in BCA, and on the hat O–C–B in EBCA. We see that the peak of the triangle is shifted from $\rho = \frac{1}{2}$ to $\rho = \frac{1}{3}$. The shift of the peak to the lower density has already been shown by Fukui and Ishibashi [12]. The reason is as follows: if states of '0' and '2' have $\rho \leqslant \frac{1}{3}$, then there are, on average, two vacant spaces in front of '2'. Thus a car can increase its velocity from 1 to 2. When ρ exceeds $\frac{1}{3}$, it cannot increase its velocity due to the full-packed sites.

Numerical experiments also show that steady states of '1' and '2' in BCA do not increase their flow when higher velocity is introduced. This is also because there are enough site '2' to block the traffic flow. Then the line A–B does not change in EBCA. Taking these facts into consideration, multiple states will appear between $\frac{1}{3} \leqslant \rho \leqslant \frac{1}{2}$ when higher velocity is introduced due to the separation of degenerated states.

4. Unstable free flow and shock wave

Let us consider in detail the new branch C–D in figure 6. We can observe that the steady state near D in C–D is unstable with respect to 'perturbation'. We give a perturbation to a

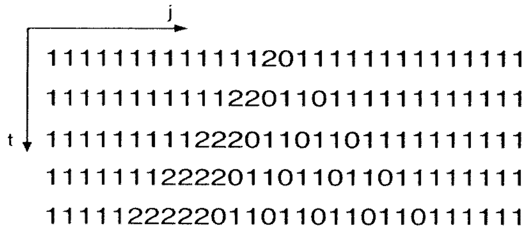

Figure 7. Time evolution of . . . 11120111 . . . by EBCA.

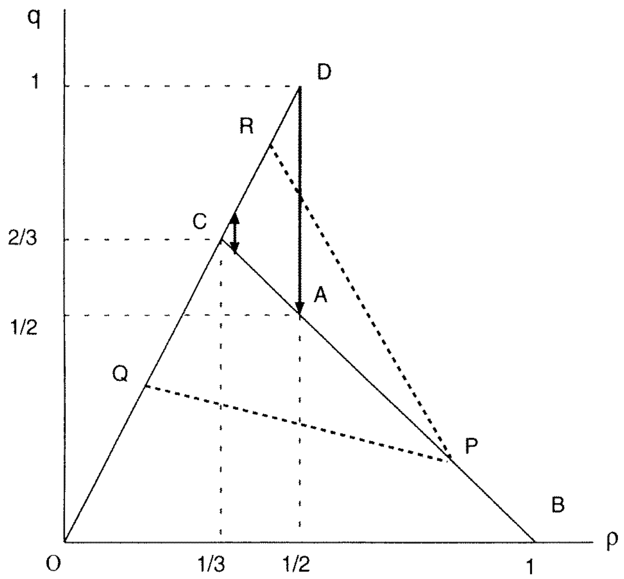

Figure 8. The schematic diagram of figure 4(*a*). States on the line *C*–*D* can transit to those on the line *C*–*A* under some perturbations.

state by shifting a car to an appropriate vacant space. Let us consider a perturbation from the state . . . 11 . . . to the state . . . 20 . . . . Physically, this means that there are at least two successive '1' sites, and the front car decreases its speed and consequently the site behind it becomes a full-packed '2' site. This perturbation apparently does not change the average car density. Time evolution of the state . . . 1111111111 . . . on D with respect to the perturbation is shown in figure 7. We can prove that the state D transits to congested state A after enough time (figure 8). From figure 7, the tail of the string 22 . . . 2 expands backwards as fast as '0' at the front advances, and the front of the string 22 . . . 2 expands backwards with half the speed. Therefore at sufficiently large t, we see that the number of '2' $\sim n$ and the number of '1' $\sim 3n \times \frac{2}{3} = 2n$. Considering that the car at site '2' cannot move and the car at the site '1' can move 2 sites ahead per time, the mean velocity from the tail of the string 22 . . . 2 to the front of '0' is

$$\langle V \rangle \sim \frac{2n \times 2}{2 \times n + 2n} \sim 1. \tag{6}$$

Of course the average car density remains $\rho = \frac{1}{2}$ during the time evolution, and the periodic boundary condition does not change the above discussions. Thus the traffic flow $q = \rho\langle V \rangle$ will eventually approach $\frac{1}{2}$.

Numerical experiments show that a state on line C–D transits to C–A under an appropriate perturbation. This means that states of free traffic flow are unstable against perturbation if car density is high ($\frac{1}{3} < \rho$). If only one car decreases its speed in this unstable state of free phase, then the whole traffic flow will eventually come into the congested phase. The existence of the unstable branch is also discussed in [22] in relation to the modified version of the Nagel and Schreckenberg model and our results have good agreement with their discussions.

Further, it is interesting to note that a state near C on C–A can transit to C–D under an appropriate perturbation as shown in figure 8. For example, let us consider the steady state 110110111110, with period $K = 12$, on C–D. If we perturb it to 110110120110, it becomes a steady state on C–A. It is clear that if we perturb the latter state to the former, we also obtain a transition from C–A to C–D. In this case the effect of the perturbation does not expand to the whole state. However, a state near A on C–A, cannot transit to C–D under a perturbation since there are too many full-packed sites. Therefore the stability of the new branch C–D is summarized as follows: states near D on C–D are unstable and those near C on C–D are stable under perturbation.

The unstable properties of new branch C–D have an important role on the time evolution of the flow. As we see in figure 5, the flow can show a damping oscillation in the transition region $\frac{1}{3} \leqslant \rho \leqslant \frac{1}{2}$. If we start from a state near D on C–D with some perturbation, then fully-packed sites will grow backward and the flow will decrease in the course of time. As we impose a periodic boundary condition in this paper, the growth of congested sites will stop and new stationary flow will appear after a while. In the formation of the new stationary flow, it is sometimes observed that the jam is partially cleared. Therefore damping oscillation of the flow is seen in the transition region.

Finally let us consider the situation where a congested state exists in a free flow. It can be inferred that boundaries which separate the congested and the free state will move like a shock wave. To make discussion easier, let us consider an infinite-site space in place of a periodic one. There exists a steady congested state . . . 121212 . . . which gives a point P and a free state . . . 010101 . . . which gives a point Q in figure 8. Let us consider an initial state where a part of the former exists in the background of the latter as shown in figure 9(a). From the time evolution of this state, we can see that the shock wave which separates the left free region and the tail of the congested region propagates backward with the velocity calculated by the slope of the line Q–P in figure 8. This is proved by considering the conservation of number of cars. The conservation law of the number of cars at a boundary between free and congested regions is given by $\rho_f(v_f + c) = \rho_j(v_j + c)$, where $\rho_f(\rho_j)$ and $v_f(v_j)$ is density and velocity of the state $Q(P)$ and c is a velocity of the boundary, i.e. the shock wave. Since flow q is defined by $q = \rho v$, we obtain $c = (\rho_f v_f - \rho_j v_j)/(\rho_j - \rho_f) = (q_f - q_j)/(\rho_j - \rho_f)$, which is the slope of the line Q–P. This holds any states between O–C and C–B and the velocity is less than -1. Also, the state of the head of P becomes the state indicated by C, and the slope C–P is -1. Thus the congested state P vanishes after a time due to the difference in velocity of both boundaries of P.

Next, we consider an unstable free state . . . 01111011110 . . . giving R in figure 8. Let us make an initial state by putting a part of . . . 121212 . . . giving P in the background of . . . 01111011110 . . . as shown in figure 9(b). In this case, the new point is that the tail of the . . . 121212 . . . region shows stagnation of car flow and the stagnation region corresponds to the state 22 . . . 22 giving B in figure 8. Moreover, the stagnation region widens in the opposite direction in the course of time. This is interpreted as follows. The unstable free flow can be considered as a state of overloading of cars. Then it is easily stagnated due to perturbations as shown above. The boundary between the regions of R and B propagates backwards with a velocity calculated by the slope of line R–B, and the boundary between the regions of B and

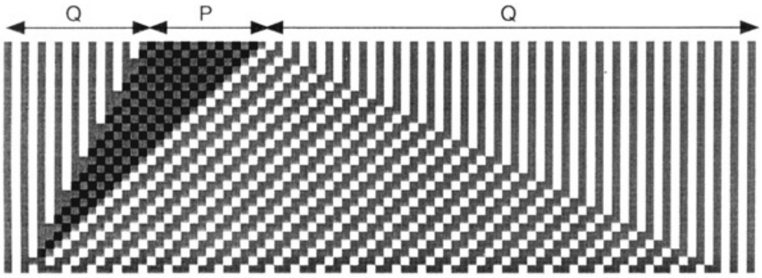

(*a*)

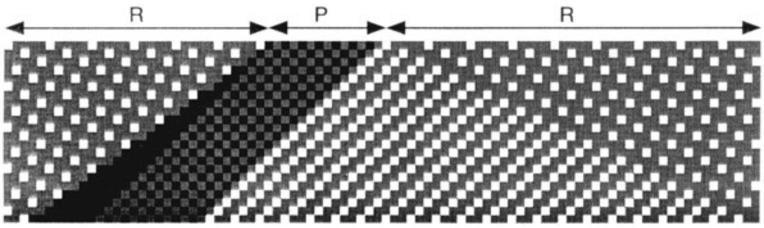

(*b*)

Figure 9. (*a*) Time evolution of a free stable region containing a congested region. The shock wave propagates backwards and the region ahead of the congested one becomes the state giving C in figure 8. (*b*) Time evolution of an unstable free region containing a congested region. The stagnation of car flow occurs behind the congested region. White, grey and black squares denote a site with value 0,1 and 2, respectively.

P moves with the velocity of the slope of line B–P, i.e. -1. Therefore the difference in the velocity of both boundaries of B will make the stagnated region wider.

Note that in both cases, we see that the head of the region of P becomes the region indicated by C in figure 8. This shows that cars do not increase their velocity to the maximum speed in the unstable region when they get out of the congested region.

5. Conclusion

We propose a new deterministic CA model of traffic flow in this paper, EBCA, which shows multiple states in the fundamental diagram. The model can be considered as the multivalue and higher-velocity generalization of rule-184 CA. A new point is that the free-moving state and the congested state coexist at $\frac{1}{3} \leqslant \rho \leqslant \frac{1}{2}$ in the fundamental diagram in the case $L = 2$, while in the case of $L = 1$ multiple states do not exist [12]. It is shown that the states in the new branch C–D transit to C–A under perturbation in figure 8. The perturbation considered in section 4 corresponds to a kind of braking. Since in the NS model braking probability is introduced as noise, then the unstable part of the new branch may disappear by introducing noise in EBCA. Introducing the influence of noise will make our model more realistic. We give the following remarks. Since our model is deterministic, analytical methods such as the ultradiscrete method [20] can be applied to study the multiple states in detail. Moreover, when we consider the general L and general V of BCA, other multiple states will appear in the diagram in the case $L \geqslant 2$, and introducing the flow limiter M in the EBCA suppresses the multiple states. Detailed analysis of these facts and of density fluctuations due to noise or open boundaries, or in comparison with other traffic flow models with metastable states will appear in succeeding papers.

Acknowledgments

The authors are grateful to Professor Hisao Hayakawa for fruitful discussions and helpful comments. This work is partially supported by Grant-in-Aid from the Ministry of Education, Science and Culture (No 9750078, 9750087).

References

[1] Greenberg H 1959 *Oper. Res.* **7** 79
[2] Kerner B S and Konhäuser P 1993 *Phys. Rev.* E **48** 2335
[3] Newell G F 1961 *Oper. Res.* **9** 209
[4] Bando M, Hasebe K, Nakayama A, Shibata A and Sugiyama Y 1995 *Phys. Rev.* E **51** 1035
[5] Bando M, Hasebe K, Nakanishi K, Nakayama A, Shibata A and Sugiyama Y 1995 *J. Physique* I **5** 1389
[6] Sasaki T and Iida Y (ed) 1992 *Traffic Engineering* (Kokumin Kagakusha) (in Japanese)
[7] Edie L C 1961 *Oper. Res.* **9** 66
[8] Navin F and Hall F 1989 *ITE Journal (August 1989)* p 31
[9] Wolfram S 1986 *Theory and Applications of Cellular Automata* (Singapore: World Scientific)
[10] Nagel K and Schreckenberg M 1992 *J. Physique* I **2** 2221
[11] Schreckenberg M, Schadschneider A, Nagel K and Ito N 1995 *Phys. Rev.* E **51** 2939
[12] Fukui M and Ishibashi Y 1996 *J. Phys. Soc. Japan* **65** 1868
[13] Fukś H and Boccara N *Int. J. Mod. Phys. C.* to appear
[14] Eisenblätter B, Santen L, Schadschneider A and Schreckenberg M 1998 *Phys. Rev.* E **57** 1309
[15] Sasvari M and Kertész J 1997 *Phys. Rev.* E **56** 4104
[16] Takayasu M and Takayasu H 1993 *Fractals* **1** 860
[17] Schadschneider A and Schreckenberg M 1997 *Ann. Phys.* **6** 541
[18] Barlovic R, Santen L, Schadschneider A and Schreckenberg M 1998 *Preprint* cond-mat/9804170
[19] Nishinari K and Takahashi D 1998 *J. Phys. A: Math. Gen.* **31** 5439
[20] Tokihiro T, Takahashi D, Matsukidaira J and Satsuma J 1996 *Phys. Rev. Lett.* **76** 3247
[21] Yukawa S, Kikuchi M and Tadaki S 1994 *J. Phys. Soc. Japan* **63** 3609
[22] Paczuski M and Nagel K 1996 *Workshop in Traffic and Granular Flow* ed D E Wolf *et al* (Singapore: World Scientific) p 73